Synaptic Dysfunction in the Hippocampus Accompanies Learning and Memory Deficits in HIV-1 Tat Transgenic Mice

Supplemental Information

Supplemental Methods

Animals and Doxycycline (DOX) Administration

Glial fibrillary acidic protein (GFAP)-driven, DOX-inducible, Tat transgenic male mice were used to evaluate the effects of the Tat protein on hippocampal structure, function and behavior. The generation of DOX-inducible, brain-specific HIV-Tat transgenic mice is described in detail elsewhere [1]. Briefly, a tetracycline (tet) ‘‘on’’ system was used for generation of inducible constructs. Tat(1–86; HIV-1_{IIIB}) was cloned downstream of a tet responsive element (TRE) in the pTREX vector (Clonetech, Mountain View, CA). The founder animals (C3H x C57BL/6J) for each construct were inbred to produce mice homozygous for the selected genes. Brain-restricted, inducible transgenic mice were created by crossing mice expressing the *tat* gene under the TRE with mice engineered to express a GFAP promoter-driven reverse tetracycline transactivator (RTTA). Pure transgenic lines were derived by crossing homologous lines containing both the GFAP-RTTA and TRE-Tat genes. In earlier studies, we validated the brain specific induction of Tat by DOX using polymerase chain reaction amplification from specific Tat primers [1, 2]. We also described constitutive (“leaky”) promoter activity that results in very low levels of tonic Tat production in Tat(+) mice without DOX induction [3]. In the present study, two groups of male mice were used: 1) control Tat(-) mice that express GFAP-RTTA but not the TRE-Tat gene, and 2) inducible Tat transgenic mice [Tat(+) mice] that express both GFAP-RTTA and TRE-Tat genes. Tat expression was induced with a specially formulated chow containing 6 mg/kg DOX (Harlan, Indianapolis, IN), fed to both control Tat(-) mice (Tat-/DOX) and inducible Tat(+) mice (Tat+/DOX) for 1-2 wk, except where indicated otherwise. DOX was administered to Tat(-) mice to control for any nonspecific actions of DOX ingestion. The 1-2 wk-

DOX exposure duration is based on findings from previously published studies that show increased astrocyte activation and an increased percentage of neurons expressing active caspase-3 in the striatum, as early as 2-d of exposure to DOX. In spite of elevations in caspase-3 [1] and increased synaptodendritic degeneration [3], neuronal TUNEL detection was unchanged in Tat+/DOX mice, even after 10 d of continuous Tat induction. These findings indicated that a 1-2 wk Tat induction is sufficient to induce synaptodendritic changes without neuronal death in the striatum, thus mimicking the types of changes seen in chronically neurocognitively impaired patients in which synaptic losses are evident in the absence of frank neuronal death. The terminology Tat+/DOX and Tat-/DOX will be used throughout the manuscript. All animal procedures were approved by the Virginia Commonwealth University of Institutional Animal Care and Use Committee and conform to Association for Assessment and Accreditation of Laboratory Animal Care International guidelines.

Assessment of Dendritic Pathology

Dendritic pathology was assessed in tissues of adult (2-3-mo old) Tat-/DOX (n = 6) and Tat+/DOX mice (n = 6). Tissues were subjected to a modified Golgi-Kopsch procedure that randomly impregnates the cell processes of neurons and glia in their entirety [4, 5]. Briefly, mice were deeply anesthetized by isoflurane inhalation and euthanatized by intracardiac perfusion with 2% potassium dichromate and 5% glutaraldehyde. Perfusion fixation was conducted at room temperature, which diminishes artifactual dendritic beading. After perfusion, whole forebrains were isolated and immersed in 2% potassium dichromate and 5% glutaraldehyde (v/v) in the dark at room temperature. The ratio of dichromate solution to tissue volume was ^{3} 50:1. After 5 d, tissues were rinsed twice in ultra-pure water three-times, blotted dry between rinses, and placed in aqueous 0.75% silver nitrate for 5 d in the dark (50:1 fluid to tissue volume ratio). Intact forebrains were infiltrated with graded sucrose solutions in 0.75% silver nitrate for 24 h intervals, embedded in Tissue-Tek O.C.T. compound (Sakura Finetek,

Inc., Torrance, CA), frozen on dry ice, and stored at –80°C. Serial, 120 mm-thick frozen sections were cut in the coronal plane, thaw-mounted on Fisher Superfrost-Plus microscope slides, dehydrated through graded ethanols, cleared in xylene, and mounted in Permount (Fisher Scientific, Waltham, MA). Non-metallic handling devices were used in all procedures. The length and morphology, and the density of spines on the apical dendrites of pyramidal neurons in the stratum radiatum of CA1 were quantified by an individual unaware of the treatment code (6-20 neurons per animal). Length of apical dendrites was measured, since afferent synapses arriving from the Schaffer collaterals (see long-term potentiation (LTP) studies below) preferentially ramify on apical dendrites within the stratum radiatum. Several criteria were used to select apical dendrites for quantification: (i) The cell must be fully impregnated throughout its entirety (partially or incompletely impregnated cells were not assessed); (ii) the dendrite must be parallel to the plane of the section: tilted/angled dendrites would foreshorten the dendrite and introduce errors in measuring the length of the dendrite; and (iii) the dendrite must be distinct from dendrites from other neurons to avoid confusion regarding to which cell the spines actually belong. Dendritic spines were assessed on pyramidal neurons in the stratum radiatum of the hippocampal field CA1. The number of dendritic spines were counted on apical dendrites, recorded as the mean number of spines per 10 mm dendrite length, averaged for each animal, and reported as changes in the mean spine density (number of spines/10 mm). Each neuron was categorized either as having dendrites with an entirely normal morphology, or having an abnormal morphology, with one or more dendrites that displayed aberrant features, such as beading and fragmentation along proximal and/or distal segments [see also 3]. The proportion of neurons that possessed one or more dendrites with abnormal morphology was counted and reported as a percentage of total neurons examined.

Cell Death Assessment

Neuron death was assessed in hippocampal tissues from 2-3-mo-old control (Tat-/DOX) (*n* = 4) and Tat+/DOX mice (*n* = 4). Twelve mm frozen sections were prepared from frozen brains, and coronal sections cut at the level of the hippocampus were collected for analysis. Specifically, four individual sections, 120 mm apart were thaw-mounted onto slides so that each slide contained representative samples from different rostral–caudal levels of the hippocampus. The slides were processed for immunohistochemistry using a monoclonal antibody to Neu-N (1:100, Chemicon) and a secondary antibody conjugated to Alexa Fluor 488 (1:500, Invitrogen). Terminal transferase-mediated UTP nick end-labeling (TUNEL) was employed to detect in situ DNA fragmentation using the In Situ Cell Death Detection Kit, TMR red (Roche Applied Science, Indianapolis, IN) in the same slides. Slides were counterstained with Hoechst 33342 (15 mg/mL; Sigma, St Louis, MO) to label cell nuclei as previously described [6-8]. To assess neuron death, the proportion of cells in which $TUNEL^+$ and $NeuN^+$ was co-detected was determined from at least 200 $NeuN^+$ cells in adjacent fields in four different sections per animal (*n* = 4), at 63x magnification. A Zeiss Axio Observer Z1 inverted microscope equipped with an MRm camera (Zeiss) was used to acquire and digitize the fluorescent images. To document nonspecific immunoreactivity, primary antibodies were either preincubated with excess antigen or omitted from the staining protocol.

Electron Microscopy

The hippocampi from 2-3-mo old Tat-/DOX and Tat+/DOX mice were prepared and processed for transmission electron microscopy (TEM). Briefly, animals were perfused with 2% paraformaldehyde/2% glutaraldehyde in neutral phosphate buffered saline (PBS) and then post-fixed in 1% osmium tetroxide (OsO_4) for 1 h, dehydrated through graded ethanol, and infiltrated overnight in EMbed 812 (EMS, Hatfield, PA). Tissue was embedded in EMbed 812 and

polymerized at 60°C for 1-2 d. Thin sections, 600-700 Å thick, were cut on the Leica EM UC6i ultramicrotome (Leica Microsystems), collected onto formvar coated grids, and stained with 5% uranyl acetate and Reynolds's lead citrate [9]. Sections were observed with a JEOL JEM-1230 TEM (JEOL USA, Inc.) and images obtained using a Gatan Ultrascan 4000 digital camera (Gatan Inc., Pleasanton, CA).

Assessment of Synaptic Vesicle-Associated Proteins

For western blotting, pre- and postsynaptic vesicle-associated protein markers were assessed in CA1 hippocampal tissues from 3-mo old control (Tat-/DOX) (n = 3) and Tat+/DOX mice (n = 3). Mice were perfused with PBS, brains were removed, and 300 µm coronal sections were cut in ice-cold DEPC-PBS with a vibratome (Microm HM 650V, ThermoFisher, Inc.). The hippocampal CA1 area was microdissected from both hemispheres of at least three brain sections and pooled per sample. Tissue was lysed in modified loading buffer containing 50 mmol/L Tris-HCl, pH 6.8, 2% sodium dodecyl sulfate (SDS), 10% glycerol, and protease inhibitors (1 mmol/L PMSF). Samples were homogenized, boiled for 10 min, centrifuged at 12,000 g for 10 min, and insoluble material was removed. Protein concentrations were determined by bicinchoninic acid protein assay (Pierce, Rockford, IL). Equal amounts of protein were loaded and separated by SDS-PAGE and transferred to PVDF membrane as described previously [10]. After blocking in 5% nonfat milk in PBS (containing 0.05% Tween20), PVDF membranes were incubated with appropriate primary antibodies, followed by horseradish peroxidase (HRP)-conjugated secondary antibodies. Immunoblotted proteins were detected with enhanced chemiluminescent detection system (ECL Plus, Amersham Pharmacia Biotech, Piscataway, NJ) as previously described [11]. Densitometry was performed using NIH ImageJ (Bethesda, MD).

Seven different monoclonal and/or polyclonal antibodies were used as pre- and postsynaptic markers in the CA1 hippocampal area. The 5 presynaptic markers included antibodies to 1) the

synaptotagmin 2 (Syt2) antibody (Mouse IgG2a, Zebrafish International Resource Center, 1:100) that detects recombinant Syt2 but not Syt1 [10], 2) the Synapsin (Syn) antibody (Mouse IgG1, Synaptic Systems, #106001, 1:100) that labels nerve terminals in mouse hippocampus [12], 3) the glutamate decarboxylase 67 (Gad67) antibody (Mouse IgG2a, Chemicon #MAB5406, 1:6000) that labels interneurons and inhibitory nerve terminals in the hippocampus [13], and 4 & 5) the vesicular glutamate transporters 1 (VGlut1, Mouse IgG1, NeuroMab; Clone N28/9, 1:400), and 2 (VGlut2, Mouse IgG1, NeuroMab; Clone N29/29, 1:400) antibodies. The 2 postsynaptic markers included 1) the postsynaptic density protein 95 (PSD-95) antibody (Mouse IgG2a, Affinity BioReagents, 1:3,000) that labels postsynaptic densities, and 2) the gephyrin (Geph) monoclonal antibody (Mouse IgG1, Synaptic Systems, 1:1,000) that labels postsynaptic structures at inhibitory synapses [14]. Finally, the mouse anti-actin monoclonal antibody (Mouse IgG1, Chemicon #MAB1501, 1:20,000) was used to normalize the data of the 7 different vesicle-associated proteins. HRP-conjugated secondary antibodies were from Jackson ImmunoResearch Laboratories (West Grove, PA) and were used at 1:10,000 dilutions.

Prompted by significant immunoblot findings, possible intraregional differences in Syt2 and gephyrin distribution were assessed by semi-quantitative measures of immunofluorescence intensity 3-mo old control (Tat-/DOX) (n = 3) and Tat+/DOX mice (n = 3). Mice were perfused with PBS and brains were removed. For Syt2 staining, one hemisphere of each animal was fixed in 4% paraformaldehyde (for 12 hours at 4°C), then washed in PBS several times and incubated for at least 24 hours in 20% sucrose in PBS, and then embedded in Tissue-Tek O.C.T. compound, frozen on dry ice, and stored at –80^{o}C. For gephyrin staining, the second hemisphere of each animal was immediately embedded in Tissue-Tek O.C.T. compound, frozen on dry ice, and stored at -80°C. For both tissues, 16-µm sections were cut on a Leica CM1850 cryostat. Sections from Tat-/DOX and Tat+/DOX mice were allowed to air dry for 15 minutes before being incubated with blocking buffer (2.5% normal goat serum, 2.5% bovine serum albumin, 0.1% Triton X-100 in PBS) for 30 minutes. Sections were incubated with primary

antibodies Syt2 (1:200) or gephyrin (1:1500), diluted in blocking buffer, for 12 hours at 4°C. After washing in PBS, the secondary antibody goat-anti-mouse Alexa Fluor 488 (1:1000, Vector Laboratories, Burlingame, CA), diluted in blocking buffer, was applied to the slides for 1 hour at room temperature. Sections were double-labeled and delineated by calbindin immunostaining. Primary mouse antibody calbindin (1:5000, Swant, Switzerland) was applied simultaneously with the primary Syt2 or gephyrin antibody, and visualization was with goat-anti-rabbit Alexa 594 (1:1000, Vector Laboratories, Burlingame, CA; 1 hour). Tissue sections were washed thoroughly with PBS, coverslipped with VectaShield (Vector Laboratories, Burlingame, CA), and visualized on a Zeiss AxioImager A1 fluorescent microscope. When comparing Tat+/DOX and Tat-/DOX samples, images were acquired by using identical parameters (i.e., identical objective, zoom, laser intensity, gain, offset, and scan speed) optimized for control tissues. Mean fluorescent intensities were determined with ImageJ without digital manipulation and converted into percentage of control. For images shown here, samples were imaged using a Zeiss LSM 700 laser scanning confocal microscope equipped with a 20x objective and a 63x oil immersion objective. Images were collected using ZEN 2009 Light Edition software (Carl Zeiss, Inc.; Thornwood, NY) and created from multiple z-slices taken through the thickness of the section, then converted into maximum projection images projected onto a single plane. Adobe Photoshop CS3 Extended 10.0 software (Adobe Systems, Inc.; San Jose, CA) was used to edit the images.

Electrophysiology

Hippocampal slices were prepared from young adult (1-mo old) control (Tat-/DOX) mice (n = 4, P22-26, 23.5 ± 0.87) and inducible (Tat+/DOX) mice (n = 4, P25-27, 26.0 ± 0.41) using standard techniques. Recordings were conducted in one slice per animal. Animals received DOX for 1-2 wk, except for one mouse that received DOX for only 3 d. The hippocampus in 1-mo old mice is considered mature with most of the synaptic connections and adult anatomical

boundaries being established during the first 1-4 wk of age [15]. It has been previously reported that the amount of LTP in adult mice (2-4 mo) is not different from that in young animals (1-2 mo) [16]. Thus, LTP and its underlying mechanisms are present at 1 mo of age and similar to adult animals. Further, conducting LTP studies in young adult mice is advantageous since the LTP responses are more robust [16] and this facilitates our ability to detect even modest effects of the *tat* gene. Recordings in young adult mice also show much slower tetanus-induced decay compared to older mice [16, 17], thereby permitting the underlying pharmacology to be more readily assessed. Each animal was anesthetized using isoflurane (AErrane, Baxter) and was decapitated soon after the disappearance of any corneal reflexes. Hippocampal slices were sectioned horizontally (400 mm-thick) and collected in oxygenated (95% O_2, 5% CO_2) ice-cold, artificial cerebrospinal fluid (ACSF in mM; 126 NaCl, 2.5 KCl, 1.25 NaH_2P04, 2 $MgCl_2$, 2 $CaCl_2$, 26 $NaHCO_3$, and 10 glucose) and gently transferred to a holding chamber. The holding chamber was placed in a 35°C warm bath for the first 30 min and then taken out of the warm bath and left at room temperature. The holding chamber was continuously superfused with ACSF and supplied with an atmosphere of humidified 95% O_2 and 5% CO_2. The composition of ACSF was (in mM) 126 NaCl, 2.5 KCl, 1.25 NaH_2P04, 2 $MgCl_2$, 2 $CaCl_2$, 26 $NaHC0_3$, and 10 glucose. Slices were allowed to recover for at least 30 min at room temperature in the holding chamber before individual slices were transferred to an interface recording chamber, where they were allowed to recover for additional 30 min. The recording chamber was continuously superfused with warm ACSF (30 ± 2°C) at a rate of 1 ml/min and supplied with an atmosphere of humidified 95% O_2 and 5% CO_2.

As depicted in Figure 4A, field potentials were measured in the stratum radiatum of CA1 using glass capillary recording microelectrodes (1.5/0.84 OD/ID, World Precision Instruments, Inc.) filled with ACSF (resistance 2-3 MW). Synaptic responses were evoked by stimulating Schaffer collaterals with 0.2-ms pulses delivered using bipolar tungsten stimulating

microelectrodes (Parylene-C insulated, Æ 125mm, 0.5 MW, A-M Systems, Inc.). Field excitatory postsynaptic potentials (fEPSPs) were recorded using an AxoClamp 2B amplifier (Axon Instruments, USA). Signals were amplified by an 8 Pole Bessel Filter (Gain: 20, Cut Off Frequency: 10 kHz, FLA-01, Cygnus Technology, Inc.) and displayed on an oscilloscope (Tektronix, Inc.). Signals were digitized (20 kHz sampling rate) using a NI BNC-2090, BNC analog adapter board for MIO E Series and PC-LPM-16 data acquisition board.

Baseline responses were obtained by stimulating the Schaffer collateral at 0.033 Hz (30 s intervals) using a stimulation intensity that yielded a half-maximal population fEPSP. fEPSP were confirmed by blocking the synaptically-evoked responses by using the competitive α-amino-3-hydroxyl-5-methyl-4-isoxazole-propionate (AMPA) receptor antagonist 6,7-dinitroquinoxaline-2,3-dione (DNQX, 20 mM, Tocris, fresh solution; bath application). LTP was assessed for 4 h after a 10 min stable baseline response. To induce LTP, one single train of high-frequency stimulation at 100 Hz (100 pulses for 1 s duration) was delivered, using the same stimulation intensity as for baseline stimulation. The fEPSP peak amplitude (mV) data were compiled using the Strathclyde Electrophysiology Software Whole Cell Analysis Program (WinWCP V3.8.2, John Dempster, University of Strathclyde, 1996-2006). fEPSP peak data were converted to percentages by setting the baseline fEPSP peak data (fEPSP before applying HFS) of the Tat-/DOX mice to 100%. Average fEPSP peak of five responses (5 x 30 s intervals = 2.5 min/interval) was calculated for further analysis.

Morris Water Maze Assessment

The Morris water maze task was used to assess spatial learning and memory in adult (2-3-mo old) control (Tat-/DOX) mice (n = 9) and in mice following Tat induction (Tat+/DOX, n = 9) over a time period of 8 d.

The Morris water maze (112 cm diameter) consisted of a plastic circular pool (112 cm diameter, 23 cm deep) filled with 21 ± 1°C water at a depth of 10 cm. The water was made opaque by the addition of nontoxic white tempera paint. The escape platform (14 cm) was located 1 cm below the surface of the water level in the center of the northeast quadrant. The pool was surrounded by two sets of cues. One set consisted of distal cues, one white background curtain at the west (W) wall, a metallic dark closet at the south (S) wall, a dark sink table of lower height at the east (E) wall, and a white wall at the north (N) wall; the second set of cues consisted of two proximal cues outside the tank perimeter, one vertical gray rectangle at the south side, and one horizontal rectangle in the north side. Performance on each trial was recorded with a camera mounted directly above the pool and analyzed with an image tracking software (Videomex-V, Columbus Instruments, Ohio).

The experiment was divided into 1-5 d acquisition training sessions to assess spatial learning, followed by one testing session 2 d later to assess spatial memory. All animals were tested in acquisition training for five sessions (1 session/day) with four trials per session. Each trial was separated by 10-15 min intervals. On each trial, the start point (NW, SW, and SE) occurred in a quasi-random manner, with each point occurring at least once per session and balanced across subjects and treatment. NE was not used as a start point because the escape platform was located in the center of the NE quadrant. A training trial began with the mice being placed into the pool using one of the entry points. The animal's swimming behavior was recorded for 60 s. If the animal was unable to locate the platform after 60 s, the trial was ended and the mouse was directed to the platform by the experimenter and allowed to remain there for 15 s. Latency (s) to find the platform, distance traveled (cm) to reach the platform, and swimming speed (cm/s) were calculated for each trial.

The probe test was conducted 2 d after the last acquisition session. During the probe test, the platform was removed and the mice were allowed to swim freely for 20 s. The average

proximity (cm) to the location of the absent target platform was determined for each mouse, while time spent in each of the four quadrants was also calculated.

Statistical Analyses

Data were analyzed using either Student *t*-tests for two group comparisons or analysis of variance (ANOVA) techniques (SYSTAT 11.0 for Windows, SYSTAT Inc.) for multiple group comparisons followed by post hoc tests, using Bonferroni's or Tukey's correction, when necessary. For the within-subjects factors (i.e., comparing multiple sessions), violations of compound symmetry were addressed by using the Greenhouse–Geisser (1959) degrees of freedom correction factor [18]. For individual time points in LTP assessment, experimental groups were compared statistically by using the paired *t*-test for within-trial effects and the unpaired *t*-test for between-group effects. An alpha level of $p < 0.05$ was considered significant for all statistical tests used. Data are expressed as the mean ± standard error of the mean (SEM).

Supplemental Results

Tat-induced Disruption of Spatial Memory

For the probe test, time spent in each of the four (target, opposite, right, and left) quadrants was assessed in addition to the proximity index. The target quadrant is defined as the quadrant in which the target platform was located during acquisition training. One-way ANOVAs were conducted on the time spent in each of the four quadrants (in percent). Results indicated that control mice spend more time in the target [$F(1, 15) = 5.45$, $p < 0.05$] and adjacent right [$F(1, 15) = 6.24$, $p < 0.05$] quadrant compared to the Tat+/DOX mice, suggesting that control Tat-/DOX mice remembered the location of the target platform much better than their Tat+/DOX counterparts and confirming the findings from the proximity index (Figure 5D).

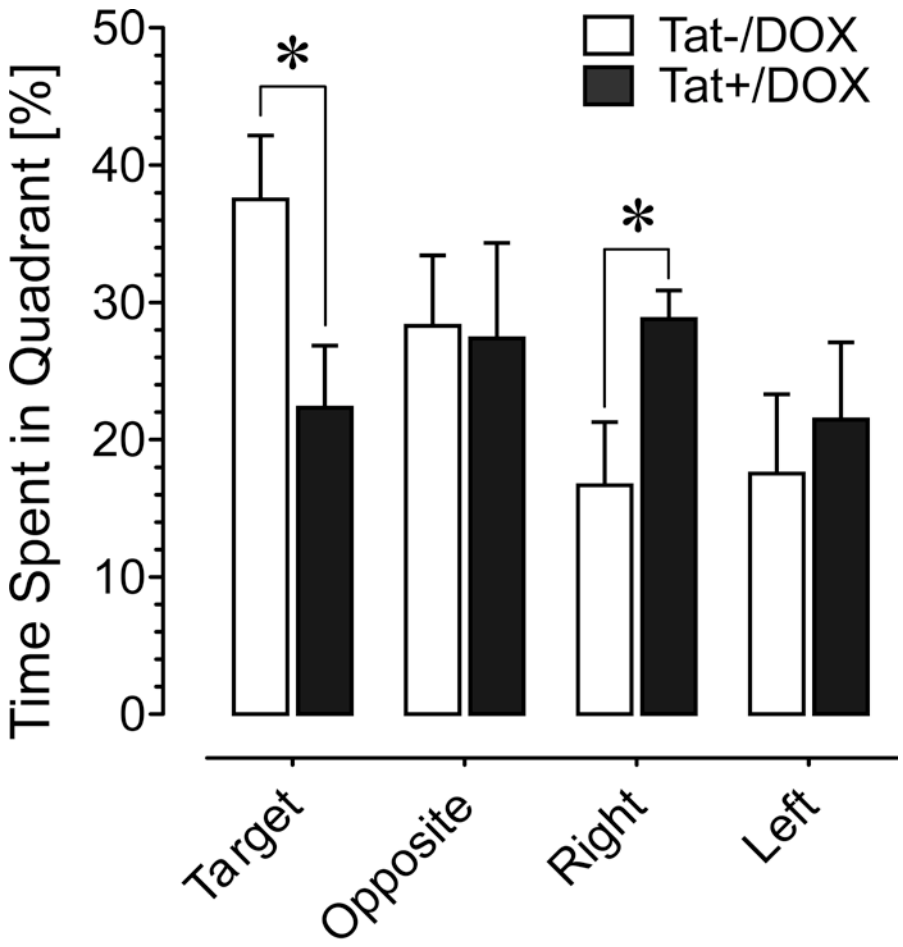

Figure S1. Effects of Tat induction in the Morris water maze in the probe test for 2-3-mo old mice. Mean (± SEM) percent time spent in the target, opposite, right, and left quadrants during the probe test (chance performance is 25%). One-way analyses of variance were conducted on the time spent in each of the four quadrants (in percent). Results indicated that control mice spend more time in the target and adjacent right quadrant compared to the Tat+/DOX mice [Tat induction effect: $F(1, 15) = 5.45$, $p < 0.05$ and $F(1, 15) = 6.24$, $p < 0.05$, respectively]. *$p < 0.05$. DOX, doxycycline.

Supplemental References

1. Bruce-Keller AJ, Turchan-Cholewo J, Smart EJ, Geurin T, Chauhan A, Reid R, *et al.* (2008): Morphine causes rapid increases in glial activation and neuronal injury in the striatum of inducible HIV-1 Tat transgenic mice. *Glia* 56: 1414-1427.
2. Duncan MJ, Bruce-Keller AJ, Conner C, Knapp PE, Xu R, Nath A, *et al.* (2008): Effects of chronic expression of the HIV-induced protein, transactivator of transcription, on circadian activity rhythms in mice, with or without morphine. *Am J Physiol Regul Integr Comp Physiol* 295: R1680-1687.
3. Fitting S, Xu R, Bull C, Buch SK, El-Hage N, Nath A, *et al.* (2010): Interactive comorbidity between opioid drug abuse and HIV-1 Tat: chronic exposure augments spine loss and sublethal dendritic pathology in striatal neurons. *Am J Pathol* 177: 1397-1410.
4. Hauser KF, McLaughlin PJ, Zagon IS (1989): Endogenous opioid systems and the regulation of dendritic growth and spine formation. *J Comp Neurol* 281: 13-22.
5. Hauser KF, Hahn YK, Adjan VV, Zou S, Buch SK, Nath A, *et al.* (2009): HIV-1 Tat and morphine have interactive effects on oligodendrocyte survival and morphology. *Glia* 57: 194-206.
6. El-Hage N, Wu G, Wang J, Ambati J, Knapp PE, Reed JL, *et al.* (2006): HIV-1 Tat and opiate-induced changes in astrocytes promote chemotaxis of microglia through the expression of MCP-1 and alternative chemokines. *Glia* 53: 132-146.
7. Bruce-Keller AJ, Chauhan A, Dimayuga FO, Gee J, Keller JN, Nath A (2003): Synaptic transport of human immunodeficiency virus-Tat protein causes neurotoxicity and gliosis in rat brain. *J Neurosci* 23: 8417-8422.
8. Bruce-Keller AJ, Umberger G, McFall R, Mattson MP (1999): Food restriction reduces brain damage and improves behavioral outcome following excitotoxic and metabolic insults. *Ann Neurol* 45: 8-15.

9. Reynolds ES (1963): The use of lead citrate at high pH as an electron-opaque stain in electron microscopy. *J Cell Biol* 17: 208-212.

10. Fox MA, Sanes JR (2007): Synaptotagmin I and II are present in distinct subsets of central synapses. *J Comp Neurol* 503: 280-296.

11. Fox MA, Colello RJ, Macklin WB, Fuss B (2003): Phosphodiesterase-Ialpha/autotaxin: a counteradhesive protein expressed by oligodendrocytes during onset of myelination. *Mol Cell Neurosci* 23: 507-519.

12. Fox MA, Sanes JR, Borza DB, Eswarakumar VP, Fassler R, Hudson BG, *et al.* (2007): Distinct target-derived signals organize formation, maturation, and maintenance of motor nerve terminals. *Cell* 129: 179-193.

13. Su J, Gorse K, Ramirez F, Fox MA (2010): Collagen XIX is expressed by interneurons and contributes to the formation of hippocampal synapses. *J Comp Neurol* 518: 229-253.

14. Henny P, Jones BE (2006): Innervation of orexin/hypocretin neurons by GABAergic, glutamatergic or cholinergic basal forebrain terminals evidenced by immunostaining for presynaptic vesicular transporter and postsynaptic scaffolding proteins. *J Comp Neurol* 499: 645-661.

15. Grove EA, Tole S (1999): Patterning events and specification signals in the developing hippocampus. *Cereb Cortex* 9: 551-561.

16. Watson JB, Khorasani H, Persson A, Huang KP, Huang FL, O'Dell TJ (2002): Age-related deficits in long-term potentiation are insensitive to hydrogen peroxide: coincidence with enhanced autophosphorylation of Ca^{2+}/calmodulin-dependent protein kinase II. *J Neurosci Res* 70: 298-308.

17. Capote J, Bolanos P, Schuhmeier RP, Melzer W, Caputo C (2005): Calcium transients in developing mouse skeletal muscle fibres. *J Physiol* 564: 451-464.

18. Greenhouse SW, Geisser S (1959): On methods in the analysis of profile data. *Psychometrika* 32: 95-112.